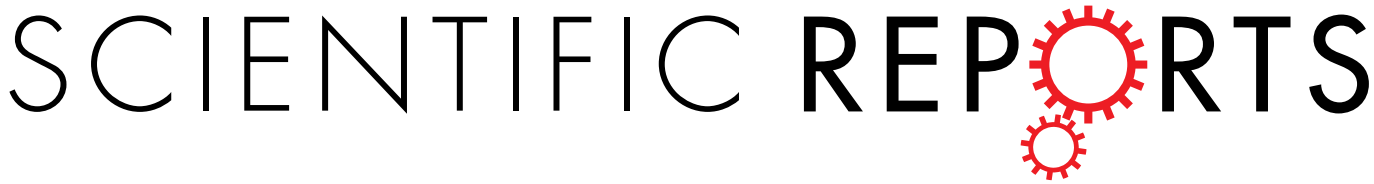

OPEN

Dephasing-Induced Control of Interference Nature in Three-Level Electromagnetically Induced Tansparency Systems

Received: 28 August 2015
Accepted: 12 October 2015
Published: 16 November 2015

Yong Sun[1], Yaping Yang[1], Hong Chen[1] & Shiyao Zhu[2,3]

The influence of the dephasing on interference is investigated theoretically and experimentally in three-level electromagnetically induced transparency systems. The nature of the interference, constructive, no interference or destructive, can be controlled by adjusting the dephasing rates. This new phenomenon is experimentally observed in meta-atoms. The physics behind the dephasing-induced control of interference nature is the competing between stimulated emission and spontaneous emission. The random phase fluctuation due to the dephasing will result in the correlation and anti-correlation between the two dressed states, which will enhance and reduce the stimulated emission, respectively.

Coherent processes based on the quantum interference in three-level media have been investigated for many years[1–11], and yielded many novel and unexpected phenomena, for example, electromagnetically induced transparency (EIT)[3–5], lasing without inversion (LWI)[6–8], and spontaneous emission cancellation[9,10]. Alkali metals in gas phase were employed in the first and many recent experiments[3,11], for their simple electronic level structure and long-lived coherence. Later experiments were also conducted with solid system, such as doped solid[12], quantum dots[13], and superconducting circuits[14]. The EIT brings the absorption cancellation (or reduction) at the resonant frequency of a transition, and gives rise to steep dispersion, as well as greatly enhanced nonlinear susceptibility in the spectral region of induced transparency of the medium[5]. Now, EIT has become a crucial technique for its potential applications such as slowing of light[15], optical storage[16], quantum information processing[17], and optical diodes[18].

Two methods, bare states and dressed states[3,5], are used in analyzing the EIT in closed three-level atoms, where a weak field probes a transition between two level and a strong field couples the upper level of the transition to the third level. In the bare state method, the absorption reduction is due to multiple pathways through the strong field coupled transition many times[19]. In the dressed state method, the EIT results from a combination of Autler-Townes splitting of the two dressed states and destructive interference in the probe absorption due to the dressed states[20]. Most of the studies on the upper-level coupled three-level atoms claim that there is only destructive interference, while for the lower-level coupled three-level atoms, most claim no interference[5,21]. Comparisons between the EIT and Autler-Townes splitting show that the quantum interference is important when the Rabi frequency of the coupling field is at the order of decay rates[21–23]. When the Rabi frequency is much larger than the decay rates, the two peaks of the absorption spectrum are well separated, and the difference between the EIT and the Autler-Townes splitting (without interference) is very small, especially for the resonance absorption. However, the influence of the dephasing on the interference nature has not been discussed. In Ref. 24,

[1]Key Laboratory of Advanced Micro-structure Materials (MOE) and School of Physics Sciences and Engineering, Tongji University, Shanghai 200092, China. [2]Beijing Computational Science Research Center, Beijing 100084, China. [3]Synergetic Innovation Center of Quantum Information and Quantum Physics, University of Science and Technology of China, Hefei, Anhui 230026, China. Correspondence and requests for materials should be addressed to H.C. (email: hongchen@tongji.edu.cn) or S.Z. (email: syzhu@csrc.ac.cn)

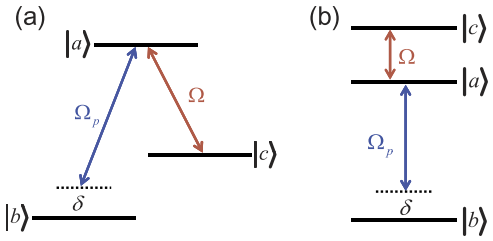

Figure 1. Three-level schemes with resonant driving. (**a**) EIT-Λ type. (**b**) EIT-cascade type. Ω and Ω_p are the Rabi frequencies of the coupling and probing fields, respectively. δ denotes the frequency detuning.

the Author gave an approximate equation under the condition of the Rabi frequency of the coupling field much larger than the decay rates, from which he found constructive (destructive) interference for lower-level (upper-level) coupled three-level atom, if the dephasing is neglected. Although, he did not explicitly discussed the transfer of the interference nature (between constructive and destructive), this equation indicates that the transfer is possible by using the dephasing rates. Furthermore, we would like to reveal the physics behind the control of interference nature.

The classical analogies of the EIT based on artificial meta-atoms recently have attracted a lot of attention[25–33] due to easy experimental demonstration and potential applications, such as slow light[25,26], low-loss metamaterial[27,28], optical storage[30], and sensing[31]. For the meta-atoms, not only the coupling strength (corresponding to the strength of the driving field), but also the intrinsic parameters of the systems can be adjusted in a relative easy way, such as the dephasing rates by using variable resistors[34,35]. Therefore, meta-atoms provide a flexible experimental platform to simulate the quantum interference phenomena in multi-level atomic systems.

In this work, we discuss the systematical control of the quantum interference nature by changing the dephasing rates in the EIT three-level system (the upper level coupled by a strong field) with the Rabi frequency of the coupling field at the order of the decay rates. Our dephasing-induced control of interference is established with the two dressed states. The dynamic equations for the two dressed states clearly show that the correlation between the two dressed states, and consequently the nature of the quantum interference, is determined by the decay rates, so that one can have constructive, destructive or no interference in the atomic absorption spectrum by simply changing the decay rates, particularly the dephasing rates. Here we also report the first experimental observation of the dephasing-induced control of the interference nature in the EIT three-level meta-atoms. The dephasing-induced transfer from constructive interference to destructive interference is demonstrated. Our results provide a clear understanding of the nature of quantum interference in three-level EIT systems, and pave a new way to control all kinds of interference by adjusting the dephasing rates.

Results

Dephasing-induced control of interference nature. Consider the upper-level coupled three-level systems, which can be EIT-Λ [see Fig. 1(a)] or EIT-cascade [see Fig. 1(b)] schemes. The three-level atom is driven by a strong field with frequency ν and Rabi frequency Ω, and is probed by a weak field with frequency ν_p and Rabi frequency Ω_p. The Hamiltonian is $H = \omega_a|a\rangle\langle a| + \omega_b|b\rangle\langle b| + \omega_c|c\rangle\langle c| - \left[\Omega_p e^{-i\nu_p t}|a\rangle\langle b| + \Omega e^{-i\nu t}|a\rangle\langle c| + c.c.\right]$. Setting $\delta = \omega_{ab} - \nu_p$ and $\Delta = \omega_{ac} - \nu = 0$ (resonant driving), the Hamiltonian in rotating frame can be written as $H = -\delta|b\rangle\langle b| - \left[\Omega_p|a\rangle\langle b| + \Omega|a\rangle\langle c| + c.c.\right]$ for the Λ scheme. The Hamiltonian for the cascade is the same with Ω replaced by Ω^*. The density matrix equations for Λ scheme in bare states are

$$\begin{aligned}
\dot{\rho}_{bb} &= \gamma_{ab}\rho_{aa} - i\Omega_p\rho_{ba} + i\Omega_p^*\rho_{ab},\\
\dot{\rho}_{cc} &= \gamma_{ac}\rho_{aa} - i\Omega\rho_{ca} + i\Omega^*\rho_{ac},\\
\dot{\rho}_{ba} &= (i\delta - \Gamma_{ab})\rho_{ba} - i\Omega_p^*(\rho_{bb} - \rho_{aa}) - i\Omega^*\rho_{bc},\\
\dot{\rho}_{ca} &= -\Gamma_{ca}\rho_{ca} - i\Omega^*(\rho_{cc} - \rho_{aa}) - i\Omega_p^*\rho_{cb},\\
\dot{\rho}_{bc} &= (i\delta - \Gamma_{cb})\rho_{bc} + i\Omega_p^*\rho_{ac} - i\Omega\rho_{ba},
\end{aligned} \tag{1}$$

where γ_{ij} is the population decay rate from $|i\rangle$ to $|j\rangle$, and $\Gamma_{ij} = \Gamma_{ji}$ is the off-diagonal decay rate of ρ_{ij}. Note $\rho_{aa} + \rho_{bb} + \rho_{cc} = 1$. The equations for the cascade scheme are the same with Ω replaced by Ω^*, and the second equation replaced by $\dot{\rho}_{cc} = -\gamma_{ca}\rho_{cc} - i\Omega^*\rho_{ca} + i\Omega\rho_{ac}$.

The imaginary part of the atomic linear susceptibility, or the absorption, is proportional to the real part of $\rho_{ab}^{(1)}/(i\Omega_p^*)$, which can be obtained by perturbation method and is the same for both schemes,

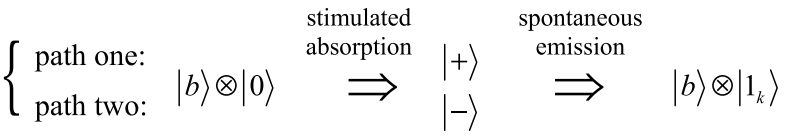

Figure 2. The interference pathways in EIT system. The two pathways, which form the interference pair, are stimulated absorption (from $|b\rangle$ to $|+\rangle$ and $|-\rangle$), and the spontaneous emission (from $|+\rangle$ and $|-\rangle$ to $|b\rangle$).

$$\frac{\rho_{ab}^{(1)}}{i\Omega_p^*} = \frac{(i\delta + \Gamma_{cb})}{|\Omega|^2 + (i\delta + \Gamma_{cb})(i\delta + \Gamma_{ab})}. \tag{2}$$

Let us consider the dressed states $|+\rangle = (|a\rangle + |c\rangle)/\sqrt{2}$ and $|-\rangle = (|a\rangle - |c\rangle)/\sqrt{2}$. The density matrix equations in the dressed states for both schemes can be obtained from Eqs. (1),

$$\dot{\rho}_{+b} = [i(-\delta + \Omega) - X]\rho_{+b} - Y\rho_{-b} + \frac{i}{\sqrt{2}}\Omega_p^*(\rho_{bb} - \rho_{++} - \rho_{+-}), \tag{3a}$$

$$\dot{\rho}_{-b} = [i(-\delta - \Omega) - X]\rho_{-b} - Y\rho_{+b} + \frac{i}{\sqrt{2}}\Omega_p^*(\rho_{bb} - \rho_{--} - \rho_{-+}), \tag{3b}$$

where $X = (\Gamma_{ab} + \Gamma_{bc})/2$, $Y = (\Gamma_{ab} - \Gamma_{bc})/2$. With the zeroth order solution $\rho_{++}^{(0)} = \rho_{+-}^{(0)} = 0$ and $\rho_{bb}^{(0)} = 1$, we can obtain

$$\begin{aligned}\frac{\sqrt{2}\,\rho_{+b}^{(1)}}{i\Omega_p^*} &= \frac{[i(\delta + \Omega) + X] - Y}{[i(\delta + \Omega) + X][i(\delta - \Omega) + X] - Y^2},\\ \frac{\sqrt{2}\,\rho_{-b}^{(1)}}{i\Omega_p^*} &= \frac{[i(\delta - \Omega) + X] - Y}{[i(\delta + \Omega) + X][i(\delta - \Omega) + X] - Y^2},\end{aligned} \tag{4}$$

and the absorption becomes $\rho_{ab}^{(1)}/(i\Omega_p) = \left(\rho_{+b}^{(1)} + \rho_{-b}^{(1)}\right)/(i\sqrt{2}\,\Omega_p)$.

If $Y = 0$, Eqs. (3a) and (3b) are two independent equations, and have no correlation between them, and Eqs. (4) tell us that the emission spectrum is a sum of two independent Lorentzian peaks with the same linewidth X and there is no interference. Y is responsible for the correlation between ρ_{+b} and ρ_{-b}, and the interference in the absorption. The energy difference between the two dressed states is 2Ω determined by the driving field. We can consider that the parameter Y, which can be written as $Y = pX$ $(-1 < p < 1)$, describes the correlation between the two effective dipole moments ($\vec{\mu}_+$ and $\vec{\mu}_-$) of the two transitions. Such dipole correlation represented by $p = \vec{\mu}_+ \cdot \vec{\mu}_- / \left|\vec{\mu}_+\right| \cdot |\vec{\mu}_-|$ will result in the quantum interference phenomenon[9]. For $Y = 0$ $(p = 0)$, we have the two dipole moments orthogonal and no interference. For $Y > 0$ $(p > 0)$, we have an acute angle between the two dipole moments, and the absorption around $\delta = 0$ is less than the sum of the two Lorentzians, which means the destructive quantum interference in the absorption. For $Y < 0$ $(p < 0)$, we have an obtuse angle between two dipole moments, and the absorption around $\delta = 0$ is more than the sum of the two Lorentzians, which means the constructive interference in the absorption. As $Y = (\Gamma_{ab} - \Gamma_{cb})/2$, we have $p = (\Gamma_{ab} - \Gamma_{cb})/(\Gamma_{ab} + \Gamma_{cb})$. We can see that Γ_{ab} and Γ_{cb} have different roles in the interference: destructive ($\Gamma_{ab} \gg \Gamma_{cb}$ and $p > 0$) and constructive ($\Gamma_{ab} \ll \Gamma_{cb}$ and $p < 0$), respectively.

As Y, which depends on the decay rates, is responsible for the interference in the absorption, it is clear that only the stimulated absorption from the lower level $|b\rangle$ to $|-\rangle$ and from $|b\rangle$ to $|+\rangle$ (from one state to two different states) could not form the pair of the interference pathways. The two interference pathways must include spontaneous decay process. Therefore, the two pathways, which form the interference pair, are stimulated absorption (from $|b\rangle$ to $|+\rangle$ and $|-\rangle$), and then spontaneous emission (from $|+\rangle$ and $|-\rangle$ to $|b\rangle$), see Fig. 2. It is the interference of the spontaneous quenching together with the stimulated absorption that makes the electromagnetically induced transparency.

For the Λ scheme we have $\Gamma_{ab} = (\gamma_{ab} + \gamma_{ac})/2 + \gamma_a^{(d)}$ and $\Gamma_{bc} = \gamma_c^{(d)}$, with $\gamma_a^{(d)}$ and $\gamma_c^{(d)}$ the dephasing rates for $|a\rangle$ and $|c\rangle$, respectively. If the dephasing rate $\gamma_c^{(d)}$ is very small compared with Γ_{ab}, we have $X \approx Y$, leading to almost complete destructive interference at $\delta = 0$. If we have very large dephasing rate $\gamma_c^{(d)}$ compared with Γ_{ab}, which can be realized by adding some collision mechanism with level $|c\rangle$ (not level $|a\rangle$), we will have $X \approx -Y$, resulting in almost complete constructive interference at $\delta = 0$. By changing the dephasing rate $\gamma_c^{(d)}$ from small to large, we can have from almost complete destructive interference to no interference, and then to constructive interference. In Fig. 3, we plot the real part of

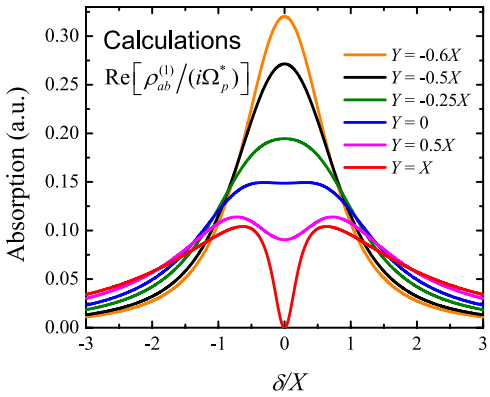

Figure 3. Calculated absorption spectra for upper-level coupled three-level system, which is proportional to the real part of $\rho_{ab}^{(1)}/(i\Omega_p)$. The magnitude of absorption at the resonance frequency gradually decreases with Y. For $Y = 0$, the absorption spectrum equals to the sum of two Lorentzian peaks with the same linewidth X (Blue). For $Y < 0$ ($Y > 0$), constructive (destructive) interference of the absorption is observed at the resonance frequency.

$\rho_{ab}^{(1)}/(i\Omega_p^*)$ for the Λ scheme with different Y from $Y = X$ to $Y = -0.6X$ with $X = 4.8$ and $\Omega = 0.63X$. The blue curve is a sum of two Lorentzians for $Y = 0$. From Fig. 3 we can see clearly the transition from complete destructive interference (red curve) to constructive interference (orange curve). Similar curves can be found for the cascade EIT scheme, from almost complete constructive ($Y \approx -X$) to almost complete destructive ($Y \approx X$) interference by changing only the dephasing rates.

We ask ourselves why Γ_{ab} and Γ_{cb} play the different roles in the interference and what is the mechanism to understand the dephasing-induced control of interference. The decay rates Γ_{ab} and Γ_{cb} are related to the population decay and dephasing of level $|a\rangle$ and $|c\rangle$, respectively. The decay Γ_{ab} is caused by population and dephasing reservoirs of $|a\rangle$, while decay Γ_{cb} is caused by population and dephasing reservoirs of $|c\rangle$. The reservoirs of $|a\rangle$ (or $|c\rangle$) result in random phase changes of $|a\rangle$ (or $|c\rangle$). The random phase changes of $|+\rangle$ and $|-\rangle$ due to the reservoirs of $|a\rangle$ are correlated by the strong field, so that the two random phase changes are of the same magnitude and the same sign because of $|\pm\rangle = (|a\rangle \pm |c\rangle)/\sqrt{2}$ (the common plus sign before $|a\rangle$). Due to the correlation of the random phase changes for $|+\rangle$ and $|-\rangle$, the system from $|b\rangle$ to $|+\rangle$ and $|-\rangle$ by stimulated absorbing a probe photon can stimulatedly emit the same probe photon with the same frequency and phase from to $|-\rangle$ and $|+\rangle$ to $|b\rangle$, which has no contribution to the absorption. It is these stimulated emission processes that prevent the spontaneous emission, so that the contribution of the reservoirs of $|a\rangle$ to the spontaneous emission is reduced or eliminated. This is why we have destructive interference. Similar discussion can be made for the reservoirs of $|c\rangle$, which will result in anti-correlation (same magnitude with opposite signs) for the random phase changes, because of $|\pm\rangle = (|a\rangle \pm |c\rangle)/\sqrt{2}$ (the opposite signs before $|c\rangle$), which leads to reduction or inhibition of the stimulated emission and enhances the spontaneous emission, so that we have constructive interference in the absorption. For $\Gamma_{ab} = \Gamma_{cb}$ ($Y = 0$), the correlation and the anti-correlation cancel each other, and we have no interference.

Experimental demonstration in meta-atoms. For an atomic system, the adjustment of the dephasing rates is limited because it is difficult to get proper parameters by direct tuning the atomic collisions[36–38]. Here we resort to the classical analog of EIT in meta-atoms to give the experimental demonstration of the dephasing-induced control of interference nature.

It has been shown that the dynamic equations for the classical EIT in meta-atoms are given as[26,33,39,40]

$$\begin{aligned}\frac{d}{dt}a_1 &= (-i\delta' - \gamma_1 - \Gamma_1)a_1 + i\kappa a_2 + i\sqrt{\gamma_1}S_{in},\\ \frac{d}{dt}a_2 &= (-i\delta' - \Gamma_2)a_2 + i\kappa a_1,\end{aligned} \tag{5}$$

where S_{in} is the input field with frequency detuning δ' which will excite the mode a_1 (but not the mode a_2), and κ is the near-field coupling strength between the two resonant modes in the meta-atom (κ's role is same as the Rabi frequency Ω in atomic EIT system). a_1 is a "bright" mode that has outputs in both forward and backward directions with a scattering loss rate γ_1, while a_2 is a "dark" mode that has no

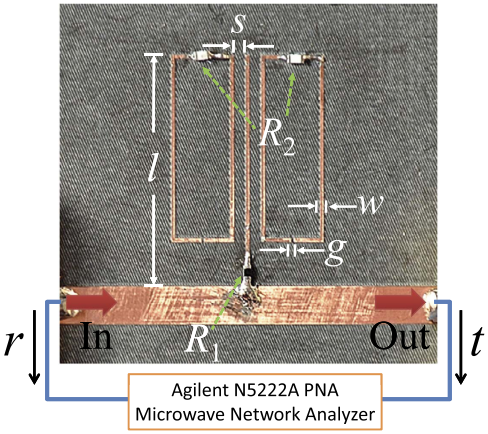

Figure 4. Experimental setup to simulate the dephasing-induced control of interference in atomic EIT system. Transmission and reflection coefficients are measured with the microwave network analyzer. The EIT meta-atom consists of a "bright" resonator, a "dark" resonator, the pair of split rings. The near-field coupling strength between the two resonators is determined by the separation s, and the dephasing rates of the two resonators, $\Gamma_{1,2}$, can be adjusted by two resistors $R_{1,2}$, respectively. Geometric parameters can be found in the Main Text.

output and no scattering loss. The two modes have the same resonant frequency, and suffer decay with different dephasing rates Γ_1 and Γ_2, respectively.

After some derivations, we obtained that

$$-\frac{r}{\gamma_1} = \frac{(i\delta' + \Gamma_2)}{\kappa^2 + (i\delta' + \gamma_1 + \Gamma_1)(i\delta' + \Gamma_2)} = \frac{(i\delta' + X' - Y')}{\kappa^2 + (i\delta' + X' + Y')(i\delta' + X' - Y')}, \quad (6)$$

where $X' = (\gamma_1 + \Gamma_1 + \Gamma_2)/2$, $Y' = (\gamma_1 + \Gamma_1 - \Gamma_2)/2$, r is the reflection coefficient, and the transmission coefficient is $t = 1 + r$. The dependence of $-r/\gamma_1$ on the decay rates of the resonant modes ($\gamma_1 + \Gamma_1$ and Γ_2) is the same as that in $\rho_{ab}^{(1)}/(i\Omega_p^*)$ on the atomic decay rates, see Eqs. (2) and (4). Therefore, the real part of $-r/\gamma_1$ corresponds to the absorption in the atomic EIT system. We can measure r versus δ' to simulate the dependence of the absorption in the atomic EIT system on δ.

Our experiments are conducted by using meta-atom in microwave range. The experimental setup is shown in Fig. 4. The meta-atom is composed of two coupled resonators. The bright resonator (a_1) is a copper branch with the length of $l = 14.9$ mm, and it is connected with the main-strip by the resistor R_1, as indicted in the middle of Fig. 4. The dark resonator (a_2) is composed of two metal split rings with the dimensions of 12 mm × 4 mm, which are located at the two sides of the first resonator. It has been demonstrated that the response of this configuration composed of the bright and the dark resonators can be regarded as the classical analogue of the EIT[26–29,34,35]. Here the width of the metal copper wires is $w = 0.2$ mm. The gap size of the two rings is $g = 0.2$ mm. The frequencies of the two resonant modes are designed to be the same at 23.56 GHz. The dephasing rates of the two resonators, $\Gamma_{1,2}$, can be adjusted by two resistors $R_{1,2}$, respectively. By putting the two resonators close to each other with a distance of $s = 0.6$ mm, we can introduce the near-field coupling κ between the two modes. When a microwave of frequency ω propagates along the main-strip (incident from the left), we have input to the bright resonator (S_{in}) which excites a_1. The dark resonator is far away from the main-strip, so that no input for the dark resonator. The dark mode a_2 is excited by the coupling between the two modes. The motion of the resonant modes is described by Eq. (5). After doing the full-wave simulations of the meta-atom with the chosen geometric parameters, we have $\gamma_1 = 2.41$ GHz, $\kappa = 7.54\ \exp(-s/0.66) = 3.04$ GHz, and $\Gamma_1 = 0.1R_1$ GHz, $\Gamma_2 = 0.05R_2$ GHz[39]. Then we can adjust R_1 and R_2 to have different Γ_1 and Γ_2.

In Fig. 5, we present the measured spectral of the real part of $(1 - t)/\gamma_1$ (rather than the equivalent quantity $-r/\gamma_1$) with different dephasing rates given by resistors $R_{1,2}$. This is mainly for two reasons: (i) Compared to the reflection coefficient r with respect of the mirror plane of the structure, the transmission coefficient t is relatively easy to measure. (ii) The slight asymmetry of the sample due to the fabrication leads to the difference between the reflections for the incident from left side and right side, while the transmissions are reciprocal and uniquely determined. Here we fix $2R_1 + R_2 = 144\ \Omega$, which makes X' be a constant, $X' = (\gamma_1 + \Gamma_1 + \Gamma_2)/2 = 4.8$ GHz, and all of the frequencies and dephasing rates are normalized with X'. By changing R_1 and R_2 simultaneously, we can make Y' from $-X'/2$ ($R_1 = 0\ \Omega$, $R_2 = 144\ \Omega$) to $+X'$($R_1 = 72\ \Omega$,$R_2 = 0\ \Omega$), that is to say, from a constructive interference to a destruc-

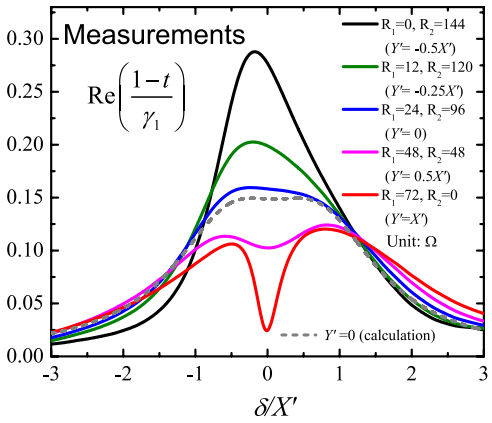

Figure 5. Measured spectral of the real part of $(1 - t)/\gamma_1$ with different dephasing rates given by resistors $R_{1,2}$. The real part of $(1 - t)/\gamma_1$ corresponds to the the real part of $\rho_{ab}^{(1)}/(i\Omega_p)$. As a comparison, the theoretical calculation for $Y' = 0$ is given with the gray dash line. Our measurements consist with the calculations in Fig. 3 reasonably well.

tive interference. The measured spectra of $\mathrm{Re}(1 - t)/\gamma_1$ in Fig. 5 show clearly the phenomenon of the dephasing-induced control of interference, namely, the transition from the constructive to the destructive interference with the increasing of Y'. For the case of $Y' = 0$ ($R_1 = 24\ \Omega$ and $R_2 = 96\ \Omega$), there is no interference, and the measured spectrum approaches to the sum of the two Lorenzians, see the blue curve (the theoretical calculation is also plotted for comparison, see the gray dashed curve), with the resonance centers $\delta' = \pm\kappa$ and the common line-width X'. Here non-zero value of $\mathrm{Re}(1 - t)/\gamma_1$ at $Y' = X'$ (red curve in Fig. 5) is due to a little inevitable dissipation from the material and the roughness. Although there is a little difference between our measurements and theoretical calculation due to the fabrication tolerance, as well as the effects from the high-order modes and the imperfect match at input/output ports (as these unfavorable factors are not considered in theoretical calculation), our experiments have no doubt simulated the constructive, destructive and no interference in EIT three-level system by adjusting only the dephasing rates in meta-atom.

Discussion

The new phenomenon, the dephasing-induced control of interference nature has been theoretical investigated and experimentally observed in the three-level EIT system. We find that the nature of the interference is dependent on the decay rates, but not related to the strength of the driving field. The random phase fluctuation due to the dephasing will result in the correlation and anti-correlation between the two dressed states, which will enhance and reduce the stimulated emission, respectively. The physics behind the dephasing-induced control of interference is the competing between stimulated emission and spontaneous emission.

Methods

The samples are all fabricated on copper-clad 0.787-mm thick Rogers RT5880 substrates using laser direct structuring technology (LPKF ProtoLaser 200). Transmission and reflection properties were obtained directly from the microwave vector network analyzer (Agilent N5222A). In addition, a commercial software package (CST Microwave Studio) is used in designing the samples.

References

1. Javan, A. Theory of a Three-Level Maser. *Phys. Rev.* **107,** 1579–1589 (1957).
2. Schawlow, A. L. & Townes, C. H. Infrared and Optical Masers. *Phys. Rev.* **112,** 1940–1949 (1958).
3. Boller, K. J., Imamolu, A. & Harris, S. E. Observation of electromagnetically induced transparency. *Phys. Rev. Lett.* **66,** 2593–2596 (1991).
4. Lukin, M. D. & Imamoglu, A. Controlling photons using electromagnetically induced transparency. *Nature* **413,** 273–276 (2001).
5. Fleischhauer, M., Imamoglu, A. & Marangos, J. P. Electromagnetically induced transparency: Optics in coherent media. *Rev. Mod. Phys.* **77,** 633–673 (2005).
6. Scully, M. O., Zhu, S.-Y. & Gavrielides, A. Degenerate quantum-beat laser: Lasing without inversion and inversion without lasing. *Phys. Rev. Lett.* **62,** 2813–2816 (1989).
7. Harris, S. E. Lasers without inversion: Interference of lifetime-broadened resonances. *Phys. Rev. Lett.* **62,** 1033–1036 (1989).
8. Scully, M. O. & Fleischhauer, M. Lasers Without Inversion. *Science* **263,** 337–338 (1994).
9. Zhu, S.-Y. & Scully, M. O. Spectral Line Elimination and Spontaneous Emission Cancellation via Quantum Interference. *Phys. Rev. Lett.* **76,** 388–391 (1996).
10. Lee, H., Polynkin, P., Scully, M. O. & Zhu, S. Y. Quenching of spontaneous emission via quantum interference. *Phys. Rev. A* **55,** 4454–4465 (1997).

11. Liu, C., Dutton, Z., Behroozi, C. H. & Hau, L. V. Observation of coherent optical information storage in an atomic medium using halted light pulses. *Nature* **409,** 490–493 (2001).
12. Longdell, J. J., Fraval, E., Sellars, M. J. & Manson, N. B. Stopped Light with Storage Times Greater than One Second Using Electromagnetically Induced Transparency in a Solid. *Phys. Rev. Lett.* **95,** 063601 (2005).
13. Marcinkevičius, S., Gushterov, A. & Reithmaier, J. P. Transient electromagnetically induced transparency in self-assembled quantum dots. *Appl. Phys. Lett.* **92,** 041113 (2008).
14. Dutton, Z., Murali, K. V. R. M., Oliver, W. D. & Orlando, T. P. Electromagnetically induced transparency in superconducting quantum circuits: Effects of decoherence, tunneling, and multilevel crosstalk. *Phys. Rev. B* **73,** 104516 (2006).
15. Hau, L. V., Harris, S. E., Dutton, Z. & Behroozi, C. H. Light speed reduction to 17 metres per second in an ultracold atomic gas. *Nature* **397,** 594–598 (1999).
16. Phillips, D. F., Fleischhauer, A., Mair, A., Walsworth, R. L. & Lukin, M. D. Storage of Light in Atomic Vapor. *Phys. Rev. Lett.* **86,** 783–786 (2001).
17. Yang, X., Zhou, Y. & Xiao, M. Entangler via electromagnetically induced transparency with an atomic ensemble. *Sci. Rep.* **3,** 3479 (2013).
18. Wang, D. W. *et al.* Optical Diode Made from a Moving Photonic Crystal. *Phys. Rev. Lett.* **110,** 093901 (2013).
19. Fleischhauer, M. *et al.* Resonantly enhanced refractive index without absorption via atomic coherence. *Phys. Rev. A* **46,** 1468–1487 (1992).
20. Zhang, G. Z., Katsuragawa, M., Hakuta, K., Thompson, R. I. & Stoicheff, B. P. Sum-frequency generation using strong-field coupling and induced transparency in atomic hydrogen. *Phys. Rev. A* **52,** 1584–1593 (1995).
21. Anisimov, P. M., Dowling, J. P. & Sanders, B. C. Objectively Discerning Autler-Townes Splitting from Electromagnetically Induced Transparency. *Phys. Rev. Lett.* **107,** 163604 (2011).
22. Giner, L. *et al.* Experimental investigation of the transition between Autler-Townes splitting and electromagnetically-induced-transparency models. *Phys. Rev. A* **87,** 013823 (2013).
23. Abi-Salloum, T. Y. Electromagnetically induced transparency and Autler-Townes splitting: Two similar but distinct phenomena in two categories of three-level atomic systems. *Phys. Rev. A* **81,** 053836 (2010).
24. Agarwal, G. S. Nature of the quantum interference in electromagnetic-field-induced control of absorption. *Phys. Rev. A* **55,** 2467–2470 (1997).
25. Papasimakis, N., Fedotov, V. A., Zheludev, N. I. & Prosvirnin, S. L. Metamaterial Analog of Electromagnetically Induced Transparency. *Phys. Rev. Lett.* **101,** 253903 (2008).
26. Zhang, S., Genov, D. A., Wang, Y., Liu, M. & Zhang, X. Plasmon-Induced Transparency in Metamaterials. *Phys. Rev. Lett.* **101,** 047401 (2008).
27. Liu, N. *et al.* Plasmonic analogue of electromagnetically induced transparency at the Drude damping limit. *Nat. Mater.* **8,** 758–762 (2009).
28. Tassin, P., Zhang, L., Koschny, T., Economou, E. N. & Soukoulis, C. M. Low-Loss Metamaterials Based on Classical Electromagnetically Induced Transparency. *Phys. Rev. Lett.* **102,** 053901 (2009).
29. Gu, J. *et al.* Active control of electromagnetically induced transparency analogue in terahertz metamaterials. *Nat. Commun.* **3,** 1151 (2012).
30. Nakanishi, T., Otani, T., Tamayama, Y. & Kitano, M. Storage of electromagnetic waves in a metamaterial that mimics electromagnetically induced transparency. *Phys. Rev. B* **87,** 161110 (2013).
31. Liu, N., Hentschel, M., Weiss, T., Alivisatos, A. P. & Giessen, H. Three-Dimensional Plasmon Rulers. *Science* **332,** 1407–1410 (2011).
32. Taubert, R., Hentschel, M., Kästel, J. r. & Giessen, H. Classical analog of electromagnetically induced absorption in plasmonics. *Nano Lett.* **12,** 1367–1371 (2012).
33. Verslegers, L., Yu, Z., Ruan, Z., Catrysse, P. B. & Fan, S. From Electromagnetically Induced Transparency to Superscattering with a Single Structure: A Coupled-Mode Theory for Doubly Resonant Structures. *Phys. Rev. Lett.* **108,** 083902 (2012).
34. Sun, Y. *et al.* Electromagnetically induced transparency in metamaterials: Influence of intrinsic loss and dynamic evolution. *Phys. Rev. B* **83,** 195140 (2011).
35. Tassin, P. *et al.* Electromagnetically Induced Transparency and Absorption in Metamaterials: The Radiating Two-Oscillator Model and Its Experimental Confirmation. *Phys. Rev. Lett.* **109,** 187401 (2012).
36. Li, H. *et al.* Electromagnetically induced transparency controlled by a microwave field. *Phys. Rev. A* **80,** 023820 (2009).
37. Luo, B., Tang, H. & Guo, H. Dark states in electromagnetically induced transparency controlled by a microwave field. *Journal of Physics B Atomic Molecular & Optical Physics* **42,** 235505–235509(235505) (2009).
38. Sargsyan, A., Sarkisyan, D., Krohn, U., Keaveney, J. & Adams, C. Effect of buffer gas on an electromagnetically induced transparency in a ladder system using thermal rubidium vapor. *Phys. Rev. A* **82,** 045806 (2010).
39. Sun, Y., Tan, W., Li, H.-q., Li, J. & Chen, H. Experimental Demonstration of a Coherent Perfect Absorber with PT Phase Transition. *Phys. Rev. Lett.* **112,** 143903 (2014).
40. Tan, W., Sun, Y., Wang, Z.-G. & Chen, H. Manipulating electromagnetic responses of metal wires at the deep subwavelength scale via both near- and far-field couplings. *Appl. Phys. Lett.* **104,** 091107 (2014).

Acknowledgements

This work was supported by the National Key Basic Research Program (973) of China (Nos. 2012CB921601, 2013CB632701, and 2011CB922001), NSAF (Grant No. u1330203) and National Natural Science Foundation of China (Grants Nos.U1330203, 11174026, 11474221, 11234010, and 11204217). YS and HC also acknowledge the support from the Fundamental Research Funds for the Central Universities.

Author Contributions

Y.S. and Y.Y. designed and carried out the experiment, while S.Z. and H.C. with the help of Y.S. worked out the theory. All authors contributed to the writing of the manuscript.

Additional Information

Competing financial interests: The authors declare no competing financial interests.

How to cite this article: Sun, Y. *et al.* Dephasing-Induced Control of Interference Nature in Three-Level Electromagnetically Induced Tansparency Systems. *Sci. Rep.* **5**, 16370; doi: 10.1038/srep16370 (2015).